

Orientational Order of Carbon Nanotube Guests in a Nematic Host Suspension of Colloidal Viral Rods

Nicolas Puech,¹ Matthew Dennison,² Christophe Blanc,³ Paul van der Schoot,^{4,5} Marjolein Dijkstra,²
René van Roij,⁵ Philippe Poulin,¹ and Eric Grelet^{1,*}

¹*Université de Bordeaux et CNRS, Centre de Recherche Paul-Pascal, 115 Avenue Schweitzer, 33600 Pessac, France*

²*Debye Institute for Nanomaterials Science, Utrecht University, Princetonplein 5, 3584 CC Utrecht, Netherlands*

³*Université Montpellier 2 et CNRS, Laboratoire Charles Coulomb, Place E. Bataillon, 34095 Montpellier, France*

⁴*Faculteit Technische Natuurkunde, Technische Universiteit Eindhoven, Postbus 513, 5600 MB Eindhoven, Netherlands*

⁵*Instituut voor Theoretische Fysica, Universiteit Utrecht, Leuvenlaan 4, 3584 CE Utrecht, Netherlands*

(Received 23 March 2012; published 15 June 2012)

In order to investigate the coupling between the degrees of alignment of elongated particles in binary nematic dispersions, surfactant stabilized single-wall carbon nanotubes (CNTs) have been added to nematic suspensions of colloidal rodlike viruses in aqueous solution. We have *independently* measured the orientational order parameter of both components of the guest-host system by means of polarized Raman spectroscopy and by optical birefringence, respectively. Our system allows us therefore to probe the regime where the guest particles (CNTs) are shorter and thinner than the fd virus host particles. We show that the degree of order of the CNTs is systematically smaller than that of the fd virus particles for the whole nematic range. These measurements are in good agreement with predictions of an Onsager-type second-viral theory, which explicitly includes the flexibility of the virus particles, and the polydispersity of the CNTs.

DOI: [10.1103/PhysRevLett.108.247801](https://doi.org/10.1103/PhysRevLett.108.247801)

PACS numbers: 61.30.Dk, 61.30.Gd, 82.70.Dd

The alignment of colloidal particles in liquid crystals has been a topic of intensive study in recent years [1–15]. Apart from scientific interest, motivation for such studies is found in the potential applications of oriented functional particles such as carbon nanotubes, metallic or semiconducting nanowires, and nanoribbons. Typically, the size of the colloidal inclusions is much greater than the size of the nematogens, i.e., the molecular building blocks of the liquid crystal. Indeed, in most common thermotropic and lyotropic liquid crystals, the nematogens are small molecules. The nematic medium can therefore be considered as a continuous matrix in which colloidal inclusions are embedded. Under these conditions, the behavior of the liquid crystal is well described by a phenomenological approach based on continuum elasticity, interfacial energy, and surface tension anisotropy. Anisotropic colloidal inclusions in conventional thermotropic nematic liquid crystals orient in response to elastic torque and surface tension anisotropy [1–5,7]. These effects are generally very strong with associated energies vastly exceeding the thermal energy $k_B T$ that drives Brownian rotation. As a consequence, anisotropic colloidal particles exhibit a degree of orientation which is greater than that of the nematogens in which they are dispersed.

Recent developments involving novel colloids and nanoparticles, including nanotubes, nanowires, nanoribbons, and liquid crystals made of particles in the colloidal size domain, raise new questions related to the ordering of colloids in liquid crystals in which the nematogens are of a size that compares with or exceeds the size of the

inclusions. Here, we report on an exploration of this new regime, by studying the case of single-wall carbon nanotubes (CNTs) embedded in a lyotropic colloidal nematic liquid crystal of fd virus particles in water. The fd virus can be seen as a semiflexible polyelectrolyte with a contour length of $L_{fd} = 0.88 \mu\text{m}$, a bare diameter of $D_{fd} = 6.6 \text{ nm}$, and a persistence length of about $P_{fd} = 2.2 \mu\text{m}$ [16]. The liquid-crystalline phases of fd virus suspensions have been studied extensively, because the fd viruses are usually considered due to their monodispersity as an ideal rod system for comparison with theory [16–21]. CNTs with an average length of about $0.3 \mu\text{m}$ [22,23], therefore shorter than the fd virus particle, are added at a small concentration to the fd virus nematic phase. The CNT colloidal stability is provided by the adsorption of suitable surfactant molecules (in our case a bile salt), which results in an overall diameter of about 2 nm for the surfactant stabilized carbon nanotubes [22,23]. Our mixture of fd virus and CNT particles of different lengths is reminiscent of the bidisperse suspensions of rigid-rodlike particles studied theoretically by Lekkerkerker and collaborators [24]. Nevertheless experimental characterization of orientational parameters in conventional bidisperse systems made of similar particles is not straightforward since the physical properties of the particles do not depend on their size. As a consequence some key features such as the distinct degree of ordering of the particles cannot be determined.

Our system of choice is quite a unique model system, because it turns out that the orientational order parameter

of the two components (CNTs and fd viruses) can be independently measured. The order parameter of CNTs can be probed by polarized Raman and photoluminescence spectroscopies [23,25,26], and that of fd virus particles by optical birefringence [27,28]. Indeed, resonant Raman scattering of CNTs and their polarization dependent response enable us to measure the CNT mean orientation at low concentrations down to the limit in which the systems do not phase separate and the inclusions do not appreciably affect the ordering of the host particles (dilute limit). The distinctive features of our system allow us to experimentally determine the order parameter of the CNTs as a function of the order parameter of the host liquid crystal, the latter being set by the concentration of the viruses. This experimental progress offers thereby an opportunity for comparisons with theories that could not be tested with other systems. Our finding that the orientational ordering of the CNTs qualitatively increases with that of the fd virus is expected. In contrast to earlier results for rodlike guest colloids dispersed in low molecular-weight liquid crystals, we show here that the degree of orientational order of the guest particles is now smaller than that of the host. Counterintuitively, this distinctive feature suggests that using host rods with increasing aspect ratio to better orient guest nanorod particles may not lead to better alignment. In addition to providing useful guidance for the controlled processing of functional composites, the present result offers a unique route towards the development of composites that combine a high degree of alignment of the matrix components while preserving some disorder of the smaller inclusions. Such a combination is of great technological interest for composites that are expected to exhibit good mechanical properties arising from the alignment of the matrix components, and electrical or thermal conductivity arising from the formation of percolated networks of the inclusions. Usually a strong alignment of the guest functional nanorods results in a loss of contact probability and thereby in a loss of electrical conductivity. In this work, the order parameter of the guest CNTs increases from 0.1 to 0.35 as the order parameter of the host viruses is increased from 0.55 to 0.75 [Fig. 1(a)]. These results are quantitatively described by a theoretical model, which includes both the flexibility of the virus and the CNT polydispersity in length.

Experimentally, the CNT dispersions were initially prepared from an aqueous suspension of single-wall carbon nanotube bundles (furnished by Elicarb batch K3778) and dispersed by bile salt surfactant (an equimolar mixture of sodium cholate and sodium deoxycholate), at the respective concentrations of 0.5% w/w CNTs and 0.5% w/w bile salts. To exfoliate the CNT bundles, sonication was applied to the suspension for a period of three hours. A purification process by selective centrifugations was subsequently performed on the nanotube suspensions. After removing nanotube aggregates by centrifugation at low speed (30 min,

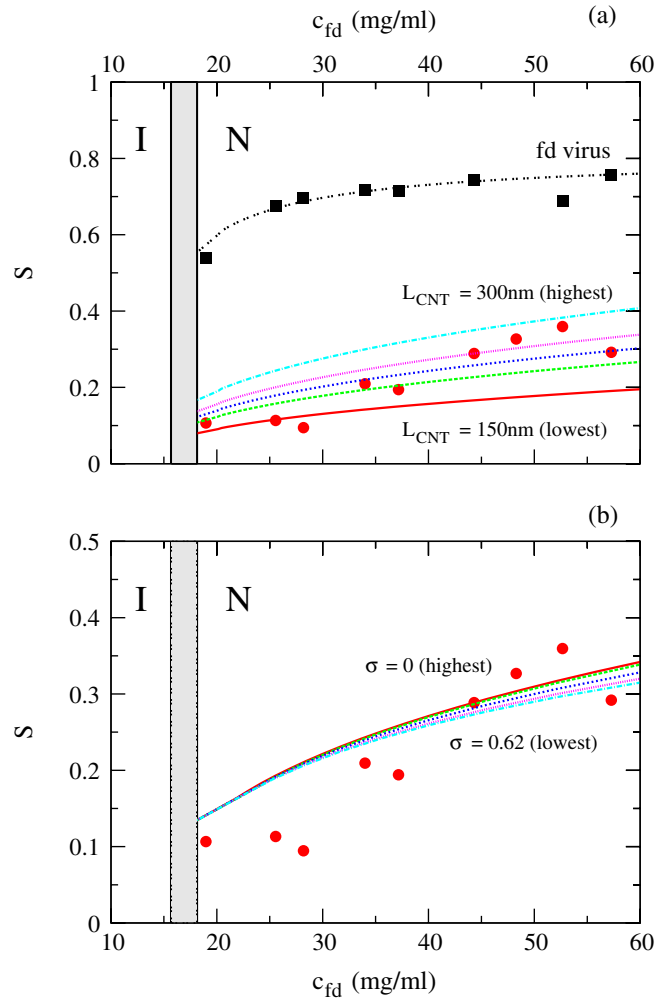


FIG. 1 (color online). Measured (symbols) and calculated (lines) orientational order parameters of the host nematic phase of fd virus suspensions S_{fd} (black squares) doped with surfactant-stabilized single wall carbon nanotubes S_{CNT} (red circles) as a function of the virus concentration c_{fd} . Theoretical results are for (a) monodisperse ($\sigma = 0$) CNTs with different lengths L_{CNT} ; (b) polydisperse CNTs with fixed average length $\langle L_{CNT} \rangle = 250$ nm and a variety of length polydispersities σ . The different lengths in (a) are L_{CNT} 150 nm (lowest line), 200 nm, 225 nm, 250 nm, and 300 nm (highest line). The different CNT polydispersities in (b) are $\sigma = 0$ (highest line), 0.13, 0.36, 0.52, and 0.62 (lowest line). The two vertical lines denote the isotropic liquid (I) and nematic (N) binodals.

2000 g), the longest carbon nanotubes exhibiting some entanglements and structural defects were removed by an ultracentrifugation step (45 min at 200 000 g). Finally, a purified surfactant stabilized CNT suspension was obtained after the last centrifugation step (180 min at 200 000 g) at a concentration of 0.34% w/w, as measured by thermogravimetric analysis. Sonication and centrifugation allow a selection of short and straight particles, which can be really considered as rigid rods, in contrast to raw and long nanotubes that exhibit a pronounced waviness or tortuosity [23].

A batch of fd virus prepared by standard biological protocols and dialyzed against a TRIS-HCl buffer at $pH = 8.2$ [16] was concentrated at $c_{fd} = 90$ mg/mL as determined by spectrophotometry, i.e., close to the chiral nematic–smectic phase transition [18]. By starting with a dispersion composed of 20% w/w of bile salt stabilized CNT dispersion and 80% w/w of fd virus suspension, further samples were prepared by mass dilution with buffer, keeping constant the fd- virus-to-CNT ratio. The samples of varying dilutions were then placed in quartz capillary tubes (0.7 mm in diameter). They were aligned first with an NMR magnet producing a field strength of about 4.6 T during 6 hours, and after that inserted in a smaller in-house made permanent magnet of about 1.5 T allowing observations with optical microscopy and spectroscopy measurements by maintaining the sample orientation. The director of the host nematic phase of virus particles aligns along the applied magnetic field, resulting in a single uniform domain. Note that CNTs exhibit a very weak magnetic anisotropy, and cannot be significantly aligned only by using an external magnetic field [29]. We found the samples to be more difficult to align for the highest concentrations in the nematic range, thereby yielding a lower alignment quality and a lower measured orientational order parameter as compared to reported values of pure fd virus suspensions [27].

Polarized Raman and polarized photoluminescence microspectroscopies were used to determine the CNT orientational order parameter, S_{CNT} . We worked with the 1064 nm line of a Nd:YAG laser and a Fourier transform Bruker RFS100 spectrometer which detects in the 900–1700 nm range. This setup allows the simultaneous measurements of the near-infrared Raman signal of all CNTs and the large near-infrared photoluminescence of individual tubes. The presence and the shape of the RBM (radial-breathing mode), G , and G' bands in the spectra (Fig. 2) are consistent with the occurrence of mainly single-wall carbon nanotubes (double-wall ones are also present in Elicarb samples but in a small proportion) [23,30]. The existence of a strong photoluminescence in these spectra with no time evolution indicates that a large fraction of the CNTs are individually well-dispersed in solution. The Raman spectra of an oriented domain, shown in Fig. 2, are obtained in the three main polarization configurations, I_{VV} , I_{HH} , and I_{VH} , where the first and second subscripts respectively refer to the polarizations of incident and scattered beams, oriented either parallel V or perpendicular H to the alignment direction, i.e., along the magnetic field. The scattered intensity in the VV configuration is much greater than the intensity for the two other ones, showing a significant orientation of nanotubes. The orientational order parameter is obtained from the intensity over all the whole studied range of wavelengths by [30]

$$S_{CNT} = \frac{3I_{VV} + 3I_{VH} - 4I_{HH}}{3I_{VV} + 12I_{VH} + 8I_{HH}}. \quad (1)$$

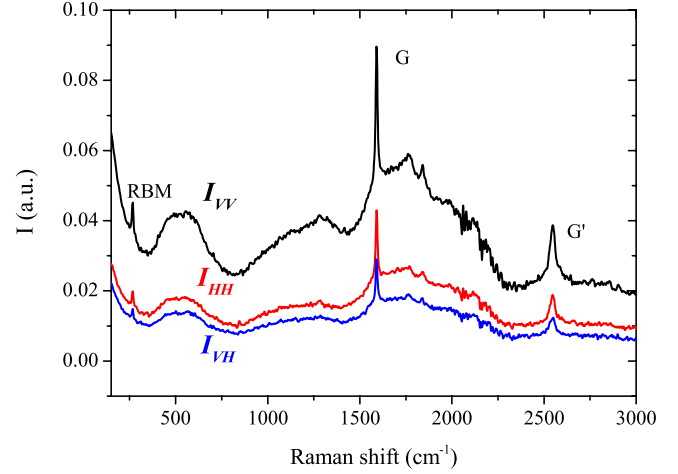


FIG. 2 (color online). Polarized Raman and photoluminescence spectra of CNTs at 0.027% w/w dispersed in a solution of fd virus at a concentration of $c_{fd} = 34$ mg/mL. The orientational order parameter S_{CNT} is obtained from the three polarization configurations I_{VV} , I_{VH} , and I_{HH} using Eq. (1). The RBM, G and G' Raman bands can be clearly distinguished.

Note that pure viral suspensions containing no carbon nanotubes do not exhibit any signal in polarized Raman spectroscopy. The orientational order parameter of the fd virus, S_{fd} , has been independently determined by optical birefringence (Δn) measurements, where the virus director field coincides with the main optical axis. The degree of alignment is given by [27]

$$S_{fd} = \frac{\Delta n/c_{fd}}{\Delta n_{sat}/c_0}, \quad (2)$$

where $\Delta n_{sat}/c_0 = 3.8 \times 10^{-5}$ mL/mg is the specific normalized birefringence of perfectly aligned viral rods [27]. Such birefringence measurements have been performed on aligned samples with the use of a Berek compensator. The very small amount of CNTs (between 0.01 to 0.06% w/w) added to the suspension of virus particles does not alter the optical properties of the sample. Moreover the use of the Berek compensator provides a direct visual measurement of the induced birefringence, which is rather insensitive to light scattering and dichroism artifacts. Indeed, the measurement does not depend on the absolute transmitted light intensity, but only on the position of the zero-order interference band minimum [31]. According to the isotropic liquid and nematic binodal concentrations and taking into account all the charged species present in solution, the ionic strength has been determined to be $I \approx 30$ mM (see Supplemental Material [32]). A set of experimental data consisting of both fd virus and CNT orientational order parameters has thus been obtained, and is presented in Fig. 1(a).

Our results are well described by using a modified Onsager theory that models the guest-host system as a binary mixture of semiflexible (fd) and rigid (CNT)

colloidal rods interacting through a hard-core excluded volume interaction (see Supplemental Material [32]). The segmented chain method described in Refs. [20,21] was used to model the semiflexible rods. We take component 1 to be the bulk fd virus liquid crystal, with the fd rod parameters (L_{fd} , D_{fd} , P_{fd}) given above. As fd virus is charged, an effective diameter needs to be introduced in the calculations, which has been defined as the diameter that gives the same coexistence densities as those found experimentally, and this is known to depend on the ionic strength [33]. Component 2 is taken to be a distribution of CNTs that are stiff, polydisperse in length, with a fixed diameter of 2 nm (see Supplemental Material [32]), and at a sufficiently low concentration so that they (i) do not interact with each other, and (ii) do not affect the density dependence of the fd virus ordering. Finally, a log-normal CNT length distribution has been used, given by

$$\Delta(l) = Cl^{-1} \exp\left[-\frac{(\ln[l] - \mu)^2}{2\omega^2}\right], \quad (3)$$

where C is a normalization factor, such that $\int dl \Delta(l) = 1$. The polydispersity is defined by $\sigma = \sqrt{\langle l^2 \rangle / \langle l \rangle^2 - 1}$, and can be expressed in terms of the mean μ and the standard deviation ω of $\ln[l]$. Here $l = L_{CNT}/L_0$ with L_{CNT} the CNT length and L_0 a reference length. For a polydisperse CNT system without fd virus, the choice of L_0 is arbitrary given sufficiently long rods [34]. In the mixture considered here, however, a length scale is set by the fd virus contour length L_{fd} , and in this case L_0 is chosen such that for a given σ we fix the mean CNT length $\langle L_{CNT} \rangle$ defined by

$$\langle L_{CNT} \rangle = L_0 \int dl \Delta(l) l. \quad (4)$$

The CNT nematic order parameter is then given by

$$S_{CNT} = \int dl \Delta(l) S_{CNT}(l). \quad (5)$$

where $S_{CNT}(l)$ is the order parameter of a CNT of reduced length l . This depends on the fd virus concentration through the orientational distribution function, and is calculated using the method given in Refs. [20,21]. The CNT length distribution has been discretized, considering 180 lengths ranging from $L_{CNT} = 50$ nm to 1000 nm, for which we found that our results have converged to the continuum limit.

In order to characterize the CNTs, we consider two cases. First, S_{CNT} is calculated for a range of $\langle L_{CNT} \rangle$ values at $\sigma = 0$, which corresponds to monodisperse CNTs dissolved in fd viruses, as a function of c_{fd} . Second, S_{CNT} has been determined for a range of CNT polydispersities σ as a function of the concentration of the background fd virus, c_{fd} . Both results are displayed in Fig. 1, which indicates that the dependence of S_{CNT} upon $\langle L_{CNT} \rangle$ is strong, whereas the results are surprisingly insensitive to the CNT polydispersity for a fixed mean CNT length $\langle L_{CNT} \rangle$.

At low c_{fd} just above the binodal, we observe that highly polydisperse CNTs with σ as large as 62% exhibit essentially the same ordering as monodisperse ($\sigma = 0$) CNTs with the same average length. At higher fd concentrations, the difference between polydisperse and monodisperse CNTs is bigger, but remains marginal. We thus reach the unexpected conclusion that the key parameter to account for the CNT ordering in the host fd virus suspension is the *average* CNT length, and *not* their length polydispersity. Clearly, this finding could largely simplify future modeling of such asymmetric hybrid systems. From our theoretical analysis, it can also be extracted that the present system is best described by $\langle L_{CNT} \rangle \sim 200\text{--}250$ nm, which is very consistent with the one expected for carbon nanotubes cut and sorted by sonication and centrifugation [22,23].

In summary, we have investigated experimentally and theoretically the coupling between the orientational order parameters of guest-host systems, in which guest carbon nanotubes are dispersed in the host nematic phase of fd virus. We focused attention on guest particles that are smaller in size than the host nematogens, preventing the description of the nematic phase as a continuum. We find that the orientational order parameter of the guest particles is lower than that of the host particles for all the studied concentrations. This implies that using probes to measure the degree of order in nematics only gives qualitative—but not quantitative—information [35]. The present results can pave the way in designing and modeling new hybrid materials with ordered nanosized and rodlike particles. In particular it conceptually provides a unique route towards the development of composites that combine mechanical strength and electrical conductivity. This combination is challenging since most available approaches to align the matrix components of a composite (such as drawing, flow induced alignment, or alignment in an external field) lead to a strong increase of the orientation of the embedded functional nanorods, being then inefficient at providing composites with both good mechanical and electrical properties. The approach developed here offers a new possibility where the main matrix components remain strongly aligned and serve as reinforcements in composites while the embedded guest nanorods preserve some disorientation as requested to achieve a high density of electrical contacts yielding a good conductivity.

This work was financially supported by ANR, FOM, and NWO-VICI grants. We thank E. Anglaret for fruitful discussions and for the use of a FTIR Raman microscope.

*grelet@crpp-bordeaux.cnrs.fr

- [1] D. Andrienko, M. P. Allen, G. Skačej, and S. Žumer, *Phys. Rev. E* **65**, 041702 (2002).
- [2] S. V. Burylov and Y. L. Raikher, *Phys. Rev. E* **50**, 358 (1994).
- [3] F. R. Hung, *Phys. Rev. E* **79**, 021705 (2009).

- [4] C. Lapointe, A. Hultgren, D.M. Silevitch, E.J. Felton, D.H. Reich, and R.L. Leheny, *Science* **303**, 652 (2004).
- [5] F. Mondiot, S. Prathap Chandran, O. Mondain-Monval, and J.-C. Loudet, *Phys. Rev. Lett.* **103**, 238303 (2009).
- [6] Z. Dogic, J. Zhang, A. W. C. Lau, H. Aranda-Espinoza, P. Dalhaimer, D.E. Discher, P.A. Janmey, Randall D. Kamien, T.C. Lubensky, and A.G. Yodh, *Phys. Rev. Lett.* **92**, 125503 (2004).
- [7] U. Tkalec, M. Škarabot, and I. Muševič, *Soft Matter* **4**, 2402 (2008); U. Tkalec, M. Ravnik, S. Čopar, S. Žumer, and I. Muševič, *Science* **333**, 62 (2011).
- [8] P. van der Schoot, V. Popa-Nita, and S. Kralj, *J. Phys. Chem. B* **112**, 4512 (2008).
- [9] I. Dierking and S.E. San, *Appl. Phys. Lett.* **87**, 233507 (2005).
- [10] S.J. Jeong, K.A. Park, S.H. Jeong, H.J. Jeong, K.H. An, C.W. Nah, D. Pribat, S.H. Lee, and Y.H. Lee, *Nano Lett.* **7**, 2178 (2007).
- [11] J.P.F. Lagerwall and G. Scalia, *J. Mater. Chem.* **18**, 2890 (2008).
- [12] M.D. Lynch and D.L. Patrick, *Nano Lett.* **2**, 1197 (2002).
- [13] G. Scalia, C. von Buhler, C. Hagele, S. Roth, F. Giesselmann, and J.P.F. Lagerwall, *Soft Matter* **4**, 570 (2008).
- [14] H.J. Shah, A.K. Fontecchio, D. Mattia, and Y. Gogotsi, *J. Appl. Phys.* **103**, 064314 (2008).
- [15] V. Weiss, R. Thiruvengadathan, and O. Regev, *Langmuir* **22**, 854 (2006).
- [16] Z. Dogic and S. Fraden, *Curr. Opin. Colloid Interface Sci.* **11**, 47 (2006).
- [17] E. Barry, D. Beller, and Z. Dogic, *Soft Matter* **5**, 2563 (2009).
- [18] E. Grelet, *Phys. Rev. Lett.* **100**, 168301 (2008).
- [19] E. Pouget, E. Grelet, and M.P. Lettinga, *Phys. Rev. E* **84**, 041704 (2011).
- [20] M. Dennison, M. Dijkstra, and R. van Roij, *Phys. Rev. Lett.* **106**, 208302 (2011).
- [21] M. Dennison, M. Dijkstra, and R. van Roij, *J. Chem. Phys.* **135**, 144106 (2011).
- [22] S. Badaire, C. Zakri, M. Maugey, A. Derré, J.N. Barisci, G. Wallace, and P. Poulin, *Adv. Mater.* **17**, 1673 (2005).
- [23] N. Puech, C. Blanc, E. Grelet, C. Zamora-Ledezma, M. Maugey, C. Zakri, E. Anglaret, and P. Poulin, *J. Phys. Chem. C* **115**, 3272 (2011).
- [24] H.N.W. Lekkerkerker, P. Coulon, R. Vanderhaegen, and R. Deblieck, *J. Chem. Phys.* **80**, 3427 (1984); R. van Roij, B. Mulder, and M. Dijkstra, *Phys. A* **261A**, 374 (1998).
- [25] C. Zamora-Ledezma, C. Blanc, and E. Anglaret, *Phys. Rev. B* **80**, 113407 (2009).
- [26] R. Saito, M. Hofmann, G. Dresselhaus, A. Jorio, and M. S. Dresselhaus, *Adv. Phys.* **60**, 413 (2011).
- [27] K.R. Purdy, Z. Dogic, S. Fraden, A. Rühm, L. Lurio, and S.G.J. Mochrie, *Phys. Rev. E* **67**, 031708 (2003).
- [28] K. Kang, A. Wilk, A. Patkowski, and J.K.G. Dhont, *J. Chem. Phys.* **126**, 214501 (2007).
- [29] M.F. Islam, D.E. Milkie, O.N. Torrens, A.G. Yodh, and J.M. Kikkawa, *Phys. Rev. B* **71**, 201401(R) (2005).
- [30] C. Zamora-Ledezma, C. Blanc, M. Maugey, C. Zakri, P. Poulin, and E. Anglaret, *Nano Lett.* **8**, 4103 (2008).
- [31] I. Dozov, E. Paineau, P. Davidson, K. Antonova, C. Baravian, I. Bihannic, and L.J. Michot, *J. Phys. Chem. B* **115**, 7751 (2011).
- [32] See Supplemental Material at <http://link.aps.org/supplemental/10.1103/PhysRevLett.108.247801> for a comparison of the chiral nematic behavior of pure virus suspension and virus suspension with CNTs as guest, and for the effect of CNT diameter and fd virus persistence length on the calculated order parameters.
- [33] J. Tang and S. Fraden, *Liq. Cryst.* **19**, 459 (1995); K.R. Purdy and S. Fraden, *Phys. Rev. E* **70**, 061703 (2004).
- [34] H.H. Wensink and G.J. Vroege, *J. Chem. Phys.* **119**, 6868 (2003).
- [35] M.P. Lettinga, C.M. van Kats, and A.P. Philipse, *Langmuir* **16**, 6166 (2000).

Supplementary Material:

Orientalional order of carbon nanotube guests in a nematic host suspension of colloidal viral rods

Nicolas Puech,¹ Matthew Dennison,² Christophe Blanc,³ Paul van der Schoot,^{4,5}
Marjolein Dijkstra,² René van Roij,⁵ Philippe Poulin,¹ and Eric Grelet^{1,*}

¹*Université de Bordeaux, Centre de Recherche Paul-Pascal - CNRS,
115 Avenue Schweitzer, 33600 Pessac, France*

²*Debye Institute for Nanomaterials Science, Utrecht University,
Princetonplein 5, 3584 CC Utrecht, Netherlands*

³*Université Montpellier 2 et CNRS, Laboratoire Charles Coulomb,
Place E. Bataillon, 34095 Montpellier, France*

⁴*Faculteit Technische Natuurkunde, Technische Universiteit Eindhoven,
Postbus 513, 5600 MB Eindhoven, Netherlands*

⁵*Instituut voor Theoretische Fysica, Universiteit Utrecht,
Leuvenlaan 4, 3584 CE Utrecht, Netherlands*

Abstract

In this Supplementary Material, theoretical results on the effects of both the CNT and fd virus dimensions on the ordering of guest CNTs in the fd virus host are first presented. Using rigid rods to describe the fd virus (i.e. $P_{fd} \rightarrow \infty$) requires the use of a much lower CNT length to find agreement with experimental results than using semiflexible rods. It is also shown that varying the diameter of the CNTs has a weak influence on their ordering, in contrast to the increase of CNT length. Furthermore, the cholesteric pitch of the fd virus host with CNTs as guest has been measured and compared with the one of pure virus suspension, confirming the validity of the dilute limit, i.e. that the CNTs do not affect the self-organization of the liquid crystalline host.

* E-mail: grelet@crpp-bordeaux.cnrs.fr

I. EFFECT OF FD VIRUS STIFFNESS

Here the effects of fd virus stiffness on the ordering of the guest CNTs is studied by varying the persistence length P_{fd} of the host fd virus. All the calculations are based on Onsager second viral theory extended for mixtures and modified to take flexibility into account through segmentation[1–3].

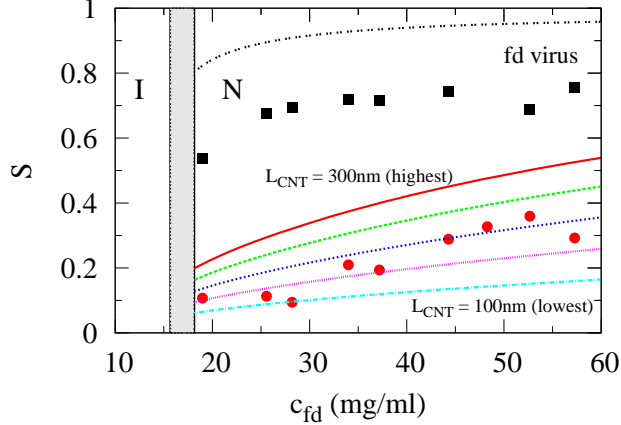


FIG. 1. Experimental orientational order parameters of the guest nematic phase of virus suspensions S_{fd} (black squares) doped with surfactant-stabilized carbon nanotubes S_{CNT} (red circles) as a function of virus concentration c_{fd} . The two vertical lines denote the isotropic liquid (I) and nematic (N) binodals. Theoretical predictions using rigid fd virus ($P_{fd} \rightarrow \infty$) and monodisperse ($\sigma = 0$) CNTs, with L_{CNT} 100nm (lowest line, light blue), 150nm (pink), 200nm (dark blue), 250nm (green) and 300nm (red) are compared. The dashed top (black) line is the calculation of S_{fd} using rigid rods ($P_{fd} \rightarrow \infty$).

Figure 1 shows the nematic order parameters of the fd virus (S_{fd}) and CNTs (S_{CNT}) for a range of CNT lengths L_{CNT} using $P_{fd} \rightarrow \infty$ (with $L_{fd} = 880\text{nm}$). The fd virus diameter is an effective one, D_{fd}^{eff} , taking into account the electrostatic repulsions between the charged viral rods: it is defined as the diameter that gives the same coexistence densities as those found experimentally. The CNT parameters are $D_{CNT} = 2\text{nm}$ and a persistence length $P_{CNT} \rightarrow \infty$. For rigid fd virus, the predicted S_{fd} is found to be much higher than that found experimentally; furthermore, the values of L_{CNT} which give the best agreement between the experimental and theoretical S_{CNT} is in this case in the range of 150 – 200nm, lower than the 200 – 250nm predicted when using semiflexible fd virus with $P_{fd} = 2.2\mu\text{m}$ and also than the experimental value of $\sim 300\text{nm}$. This is likely due to the much larger order

parameter of the rigid fd virus, which results in a larger CNT order parameter for a given set of CNT features. Clearly, incorporating flexibility into the model system is important for a quantitative description.

II. INFLUENCE OF CNT DIAMETER

The effects of CNT diameter on the order parameter of CNTs in a host fd virus solution is now examined.

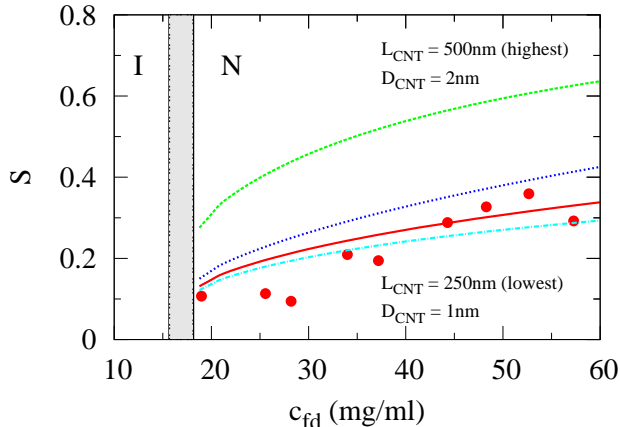


FIG. 2. Orientational order parameter of the guest carbon nanotubes S_{CNT} (red circles) in the host nematic phase of fd virus as a function of virus concentration c_{fd} . The two vertical lines mark the isotropic liquid (I) and nematic (N) binodal concentrations. Theoretical predictions for monodisperse ($\sigma = 0$) CNTs, with $L_{CNT} = 250\text{nm}$ and $D_{CNT} = 1\text{nm}$ (lowest line, light blue), $D_{CNT} = 2\text{nm}$ (red), $D_{CNT} = 4\text{nm}$ (dark blue), and with $L_{CNT} = 500\text{nm}$ and $D_{CNT} = 2\text{nm}$ (top line, green) are compared.

Figure 2 shows the evolution of S_{CNT} for four different cases: the first test case is performed with the following CNT features $L_{CNT} = 250\text{nm}$ and $D_{CNT} = 2\text{nm}$. The three other probed cases are: one using twice the CNT length ($L_{CNT} = 500\text{nm}$ and $D_{CNT} = 2\text{nm}$), one with twice the CNT diameter ($L_{CNT} = 250\text{nm}$ and $D_{CNT} = 4\text{nm}$), and one using half the CNT diameter ($L_{CNT} = 250\text{nm}$ and $D_{CNT} = 1\text{nm}$). For this study, the standard fd virus parameters are used, with $P_{fd} = 2.2\mu\text{m}$. As can be seen, doubling the CNT diameter for a fixed length has a much smaller effect than doubling the CNT length for a fixed diameter (which actually results in a smaller increase in the CNT volume than doubling the diameter).

Furthermore, halving the CNT diameter results in only a small decrease in the predicted order parameter. It is therefore apparent that, while there is some leeway when fixing the CNT diameter in any theoretical calculation (as a small difference will not strongly affect the results, and therefore only a rough estimate of the diameter is required), the key parameter for accurate predictions of CNT ordering is the CNT length.

III. CHIRAL NEMATIC PHASE

In order to experimentally prove the validity of the dilute limit used in this work, i.e. that the CNT guest does not disturb the physical properties of the fd virus host, the twist periodicity (or cholesteric pitch) of the chiral nematic host phase was measured, and compared with the pure fd virus suspension in absence of CNT. Indeed, it has been previously reported the high sensitivity of helical features like the cholesteric pitch with physicochemical parameters, such as the ionic strength [4–7].

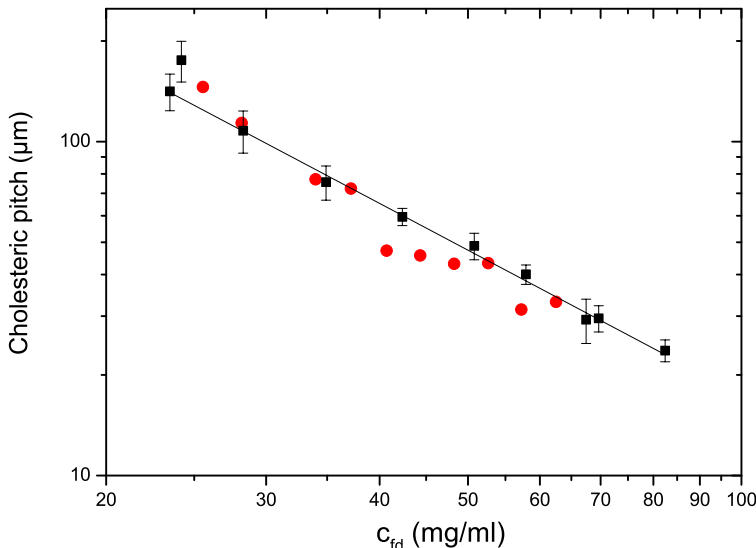


FIG. 3. Cholesteric pitch of pure virus suspension at a given ionic strength of $I=30\text{mM}$ (black squares, fitted with a power law represented by the black line) and of a guest virus suspension (red solid circles) doped with surfactant-stabilized CNT guest.

The same samples used for measuring the orientational order parameters (See main text) have been investigated for the cholesteric pitch determination. However, the absence of magnetic field to induce a nematic monodomain allows here the winding of the nematic

phase into a cholesteric one. The pitch measurements performed by polarizing microscopy [4, 5] are reported in Fig. 3, both for virus suspensions in a TRIS-HCl-NaCl buffer at 30mM and for the surfactant-stabilized CNTs dispersed in the viral liquid crystalline host. A very good agreement is found between the two systems, confirming the validity of the dilute limit used in this work, i.e. that the presence of the CNT guest with a concentration lower than 0.1% w/w does not affect the physical properties of the host mesophase of fd virus.

-
- [1] P. P. F. Wessels and B. M. Mulder, *Soft Mater.* **1**, 313 (2003); *J. Phys. Condens. Matter* **18**, 9335 (2006).
 - [2] M. Dennison, M. Dijkstra and R. van Roij, *Phys. Rev. Lett.* **106**, 208302 (2011).
 - [3] M. Dennison, M. Dijkstra and R. van Roij, *J. Chem. Phys.* **135**, 144106 (2011).
 - [4] Z. Dogic and S. Fraden, *Langmuir* **16**, 7820 (2000).
 - [5] E. Grelet and S. Fraden, *Phys. Rev. Lett.* **90**, 198302 (2003).
 - [6] F. Tombolato, A. Ferrarini, and E. Grelet, *Phys. Rev. Lett.* **96**, 258302 (2006).
 - [7] E. Barry, D. Beller and Z. Dogic, *Soft Matter* **5**, 2563 (2009).